Investigating the impact of multi-rotor structure shadowing on tidal stream turbine performance

B. Townley, W. Shi, Q. Xiao, A. Angeloudis, I. Ashton, and B. Wray

Abstract—**As the tidal stream energy sector develops, reducing the Levelised Cost of Energy (LCOE) is essential to sustain commercialisation. Modular multi-rotor foundations, with bi-directional turbines, reduce offshore operational complexity through smaller turbine diameters and lift weights, in turn reducing the device Operational Expenditure (OpEx). With the introduction of modular, multi-rotor foundations, the wake-induced impacts that these structures have on turbine performance must be investigated to better estimate energy yield, loading, and fatigue life. This study sets the scene for investigating the relationship between the turbulent wake generated by a modular ballast weighted foundation and 2-bladed Horizontal Axis Tidal Turbine (HATT) motivated by the HydroWing multi-rotor device concept. The presented work aims to determine the broader magnitude and severity of the loads and establish a transparent and well-defined methodology to be followed with further high-fidelity modelling. Initially, a transient RANS Computational Fluid Dynamics (CFD) simulation environment with a sliding mesh is configured and validated against experimental data. A turbine in free-stream isolation is simulated as a benchmark case with the modular foundation sequentially introduced to analyse the impact of the structure. Key findings suggest that operating turbines downstream of the multi-rotor foundation could cause a $\approx 20\%$ fluctuation in thrust loading at a 1.82 Hz frequency resulting in a mean C_P reduction of $\approx 8\%$ over a revolution.**

Index Terms—**Multi-rotor, tidal, CFD, RANS, turbine, thrust loading.**

This work was supported by the EPSRC and NERC through the IDCORE programme.

B. Townley is an IDCORE Research Engineer sponsored by HydroWing, Unit 3 Penstraze Business Centre, Penstraze, Truro, UK, TR4 8PN (e-mail: bryn.townley@ed.ac.uk).

W. Shi is a Reader in Net Zero Maritime Systems in the Mechanical Engineering and Marine Technology department at Newcastle University, Newcastle upon Tyne, UK, NE1 7RU (e-mail: weichao.shi@newcastle.ac.uk).

Q. Xiao is a Professor in Naval Architecutre, Ocean and Marine Energy at the University of Strathclyde, Glasgow, UK, G1 1XQ (e-mail: qing.xiao@strath.ac.uk).

A. Angeloudis is at the School of Engineering at the University of Edinburgh, and within the Institute for Infrastructure and the Environment, Edinburgh, UK, EH9 3FG (e-mail: a.angeloudis@ed.ac.uk).

I.G.C. Ashton is a Senior Lecturer in Offshore Technology in the Department of Engineering at the University of Exeter, Penryn, UK, TR10 9FE (e-mail: I.G.C.Ashton@exeter.ac.uk).

B. Wray is a Project Engineer at HydroWing, Unit 3 Penstraze Business Centre, Penstraze, Truro, TR4 8PN, UK (e-mail: brw@inyanga.tech).

Digital Object Identifier:
https://doi.org/10.36688/ewtec-2023-283

I. Introduction

Tidal stream energy developers are seeking new ways to reduce their Levelised Cost of Energy (LCOE). In the UK this is motivated by competitions for funding in one of the UK Government Contracts for Difference (CfD) allocation rounds that subsidise investments into low carbon energy options. Improving reliability and reducing maintenance complexity has been identified as a possible route to achieving this by reducing the Operational Expenditure (OpEx). One method adopted by many developers is to use multi-rotor devices, where multiple turbines are housed on the same platform in order to simplify operational challenges such as deployment, installation, maintenance, and recovery. Additionally, increasing overall reliability through fewer active components such as yawing and pitching mechanisms is being considered, which often means that these multi-rotor structures are in a fixed position throughout their life. A multi-rotor device is typically made up of multiple smaller diameter turbines, with a similar overall device capacity as a single larger diameter turbine, but with improved Operations and Maintenance (O&M). This change in design philosophy has the potential to significantly reduce costs for developers.

Understanding turbine behaviour and performance across different conditions is crucial when making decisions on which foundation or platform to deploy. In Ref. [1], J. McNaughton et al. conducted a set of tests at the University of Edinburgh's FloWave facility on designing for constructive interference to improve array performance. It was observed that for an additional 10% in thrust loading, a 20% increase in power coefficient, C_P, could be achieved by placing two turbines adjacent to each other, if blades were designed for constructive interference. It was also observed that increasing the Tip-Speed Ratio (TSR) of one of the turbines resulted in an increase in performance of the second adjacent turbine. Sequentially, in Ref. [2], J. McNaughton et al. conducted flume tank testing on a multi-rotor tidal fence to investigate the impact of turbine tip spacing on performance and loading. They observed that through reducing turbine tip spacing to 0.25D, inducing high local blockage ratios, a 1.4% overall performance increase can be obtained. Their work also characterised blade thrust loading fluctuations over a revolution for multi-rotor turbines, and highlighted the difference in loading patterns for

inboard and outboard turbines. Both of these tests demonstrate that utilising high local blockage ratios in channelled flow conditions can lead to favourable performance coefficient improvements for multi-rotor tidal arrays.

D. R. Noble et al. also conducted tank tests on an array of 3 turbines and measured blade loading and turbine power output, in Ref. [3]. Analysis was conducted on the turbine performance, and flow characteristics in both the frequency and time domain. The frequency domain analysis clearly highlighted the $1p$ and $3p$ peaks for their 3-bladed devices due to turbine rational velocity and tower shadowing effects, which can be used in the validation of future modelling work. It was observed in Ref. [3] that for a staggered array of 3 turbines, the performance of the rear turbine could be improved by up to 10% for a 5-7.5% increase in thrust loading, similarly to the findings in Ref. [1].

Numerical modelling methods can also be used as a cost-effective tool for research and design of turbine performance. In Ref. [4], a generalised actuator disk computational fluid dynamics (GAD-CFD) model was developed, which utilises a computationally efficient porous disk representation of a turbine for array optimisation. The GAD-CFD model was extensively validated against datasets from the physical tank test experiments of the 3 turbine array in Ref. [3]. Actuator disk modelling in CFD can efficiently represent turbine performance at significantly reduced computational cost as compared to fully resolved sliding mesh simulations of the rotor and blades. However, C. E. Badoe et al. stated in Ref. [4], that actuator disk modelling leads to over predictions of the performance coefficients in the over-speed tip-speed-ratio (TSR) range of the turbine.

Higher fidelity blade-resolved CFD can model dynamics which are not possible to capture with time averaged actuator disk modelling alone, but come at a much greater computational expense due to the large number of mesh cells required to resolve the boundary layer at the blade walls. In Ref. [5], I. Afgan et al. conducted 3D blade-resolved CFD simulations on a 3-bladed turbine comparing both a RANS and LES turbulence model to experimental data. It was observed in Ref. [5], that LES showed good agreement with the experimental data for low TSR flows where RANS would underpredict. They also noted that LES may fully resolve vortex shedding interactions between turbine blades and the support tower, and capture fluctuating loads on the blades, which are otherwise largely left unresolved in their RANS modelling. This greater accuracy in modelling comes at a much larger cost however, and I. Afgan et al. noted that the LES CFD model required approximately 30 times the number of CPU hours to conduct the full simulation relative to the RANS CFD model.

For tidal turbine applications, a balance must always be struck between ensuring sufficient modelling accuracy considering the problem at hand, and taking every effort to reduce complexity and cost. RANS CFD has demonstrated accuracy in modelling blade loads and turbine performance coefficients at an attainable cost. In Ref. [6], C. Frost et al. used a combination of steady-state moving reference frame (MRF) and transient sliding mesh RANS SST models to investigate the impact that a monopile support tower has on turbine performance in both an upstream and downstream configuration. MRF is a modelling technique whereby the coordinate system around a turbine is rotated at the turbines desired rotational velocity to approximate turbine revolution. The advantage of MRF is that it does not require a sliding mesh and can be used as part of a steady-state simulation, yielding significant cost savings. This particular study considered cases where the turbine tower was upstream and then downstream of the rotor. As stated in Ref. [6], bi-directional turbines provide a cost-effective and simple alternative to a yawing mechanism. Yawing devices in tidal energy devices undergo higher loads than wind turbines due to the increased fluid density, increasing complexity, cost, and maintenance requirements. The benefits a yawing system provide must therefore be significant. In their model, the turbine support tower extended the entire depth of the water column. The turbine was a 3 bladed, 10 m diameter turbine, housed on a 2.4 m diameter tower. The rotor was offset 1.8 m from the tower. In the worst case when the turbine was downstream of the monopile support tower, a 30% drop in C_P was observed relative to an unimpeded flow case. Also, the turbine experienced a $10\times$ greater blade loading magnitude when the turbine was downstream of the tower compared to unimpeded flow. This fluctuation in loading between the ebb and flood tide could have significant impacts on blade fatigue life, and C. Frost et al. recommended that the benefits of yawing mechanisms are considered in Ref. [6].

The tower shadow is an important consideration when designing multi-rotor tidal devices. A turbine in the wake of another turbine or structure will experience both reduced power coefficient (C_P) and increased dynamic loading across the blades due to the non-uniform wake velocity and turbulence intensity (TI) [7]–[9]. This is termed shadowing.

High shear stresses at the wake interface can also reduce the fatigue life of a rotor [10]. It is likely that many multi-rotor tidal developers who choose to use non-yawing turbines will suffer from shadowing as their turbines operate downstream of their support structure every other tidal cycle. The wake from the support structure housing upstream of a turbine is expected to reduce the turbine performance. In the wind energy domain where horizontal axis devices are prevalent, B. Sanderse et al. in Ref. [9], investigated the interaction between rotor performance and tower shadowing for an upstream wind turbine and found that the presence of the tower caused a 2% drop in torque and thrust on the upstream rotor [11]. Z. U. Rehman et al. then conducted a similar study using CFD on the impact a tidal turbine support tower has on rotor performance for different tower diameters, in Ref. [12]. The fluctuation of C_P through each revolution as the blades passed in front of the tower was plotted. In the worst case, they obtained a similar result as in Ref. [9] and noted a 2% drop in C_P each time the

blades approached and passed the tower. In both of these studies, the turbine tower was downstream of the rotor, and thus a minimal, but not insignificant impact on the rotor performance was observed.

B. Guo et al. in Ref. [13] conducted a similar study as in Ref. [6] and arrived at similar conclusions. The turbine tower detrimentally effects the turbine performance and generates a wake which induces fluctuating loads on the blades as they pass behind the tower. When the turbine is 1.5 diameters downstream of the tower, a 7% drop in C_P is observed. The average C_P when the turbine was downstream of the rotor was 0.405 and fluctuated between 0.352 and 0.428, highlighting the scale of the dynamic load applied to the rotor in the tower wake through each revolution. It was thus hypothesized that such fluctuations will detrimentally harm the lifespan of the turbine, increasing the dynamic loading and fatigue wear.

M. Reiso et al. compared the unsteady wake behaviour behind a monopile and a truss wind tower via a 2D CFD study fitted to the Powles' model at different flow misalignment angles, and cross sections along the tower, in Ref. [14]. The 2D study was achieved by taking representative cross-sectional planes of the multi-rotor foundation at locations of interest. The 2D truss towers were modelled at 0° and 22.5° flow misalignment. Both truss towers had a wider wake than the monopile foundation, and a higher turbulence intensity at the turbine location. The largest velocity deficit was recorded behind the truss towers rather than the monopile foundation, as one might assume. The authors stated that this was likely due to the interactions between the struts and the main beam connections increasing the deficit due to the closely spaced cylinders. The authors of Ref. [14] suggested that the main contributing factors for blade fatigue were the velocity deficit and the turbulence, rather than the unsteady vortex shedding, which had a smaller contribution to overall fatigue.

The importance of understanding the impact of support structure shadowing effect on turbine performance in both upstream and downstream configuration increases as more tidal developers consider these multi-rotor devices. We seek to build on the body of work already carried out on the subject of tower shadowing to consider case study examples from current tidal developers, and conduct higher fidelity modelling to capture the nuances of this interaction between support tower and turbine in the form of vortex shedding and fluctuating loads.

This paper sets out the initial investigation and model-based research completed relying on a 3D RANS CFD model that exploits symmetry plane to simulate adjacent turbines operating downstream of their supporting tower with the goal of examining key interactions between turbines and their support structures.

A. Case Study: HydroWing

To ensure the applicability of this research, strong links with industry are formed from the beginning.

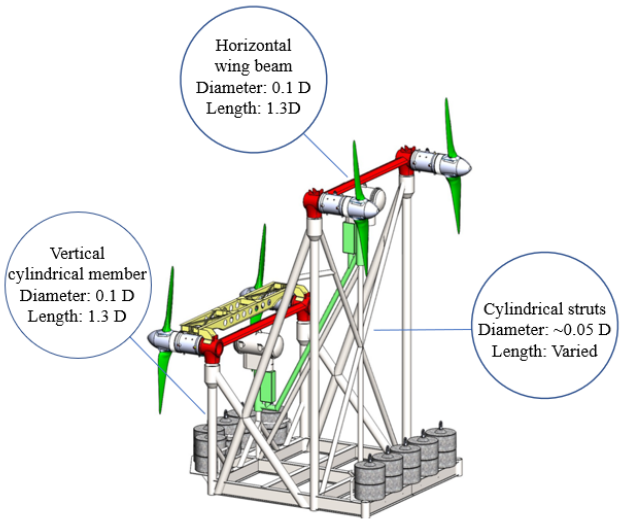

Fig. 1. Annotated HydroWing multi-rotor device concept design.

The HydroWing multi-rotor concept device serves as a case study for this research project so that research questions align with current industrial challenges. The HydroWing device, Fig. 1, is designed to simplify and de-risk tidal energy's O&M. The HydroWing concept uses Tocardo 250 kW T2si turbines, with 2 turbines mounted onto each wing. Tocardo turbines are non-yawing, and feature a passive bi-blade system, whereby the turbines pitch about their axis 180° to face the oncoming tide. The horizontal beams which connect to the turbines, referred to from here on out as the 'wings', can be seen in red in Fig. 1. These are retrievable beams with wet mate connectors to mount onto the foundation. The device wings are horizontally and vertically staggered featuring the uniquely patented flow and lift corridors. This lift corridors enable each wing to be retrieved from the sea surface for O&M, whilst the flow corridors allow for each set of wing mounted bidirectional turbines to operate in each tidal cycle outside of eachothers wakes.

II. Methodology

A. Study Objective

Multi-rotor structures often have a more complex design, and a larger footprint when compared with monopile foundations. Each strut will generate its own wake, and the turbine blades, subject to the rotor position, may interact with each of these wakes at a frequency depending on its angular velocity. In high Reynolds flow environments, such as typical ocean conditions, these beams and struts will also shed vortices onto the turbine blades and inducing additional vibrations through the foundation structure. Fig. 1 displays the HydroWing device geometry being considered. The turbines are 2-bladed, and have passive bidirectionality, so that they can operate in both the flood and the ebb tide, whilst also eliminating the need for a yawing mechanism. This adds another unique element to the problem as each turbine will operate for half of each tidal cycle in clean open flow, and operate

for the other half in the direct shadow of its multi-rotor foundation. This means that each individual turbine may experience significantly different loading patterns between each tide cycle, varying in frequency and magnitude. The scale of this difference, and its impact on fatigue life, and turbine performance are currently unknowns that this study seeks to address.

The HydroWing device was split into separate components, and then their geometry was generalised to increase the applicability of this study for other devices. Additionally, the device was simplified to investigate only a single wing tier with 2 turbines attached. The main device components are the turbines which are supported by vertical cylindrical beams, the horizontal wing beam, and then the various struts included to improve structural integrity and robustness. The wing's geometry and diameter were made equal to that of the diameter of the vertical beam (Fig. 1, vertical cylindrical struts in white). The wing and the vertical beam were identified as the two main components of interest, as the turbines are mounted to the corner of these two beams so that the blades are directly subjected to their shadow. Although an integral component to the overall structure, for this analysis the struts and cross braces were removed to simplify the modelled geometry. These struts would be of lesser diameter, and also cross the swept area of the turbines at varying angles. Removing these components simplifies the scope of the study, without impacting its applicability, and also allows for future work to investigate the impact that these struts have via a comparative study with this paper.

B. Computational Fluid Dynamics

1) Operating Conditions: The simulations are all conducted at the turbines peak C_P TSR and flow speed. This point along the power curve is different to the max power point, but is a more consistent operating condition to conduct these simulations.

The main parameters of interest are the generated turbine torque, and thrust loads. Thrust is monitored for each blade, the nacelle, and the foundation, and is the main parameter used to compare between models. Torque is used to monitor power output and C_P of the turbines. The TSR, Power Coefficient, and Thrust Coefficient are defined in (1), (2), and (3).

$$TSR = \frac{\omega R}{U} \tag{1}$$

$$C_P = \frac{\tau \omega}{0.5 \rho A U^3} \tag{2}$$

$$C_T = \frac{T}{0.5 \rho A U^2} \tag{3}$$

Where ω is the angular velocity in rad/s, R is the radius in m, U is the free-stream fluid velocity in m/s, τ is the torque in N-m, ρ is the fluid density in $\mathrm{kg/m^3}$, and A is the turbine swept area in $\mathrm{m^2}$. The free-stream velocity is taken as 2 m/s, and fluid density used is 1025 $\mathrm{kg/m^3}$.

TABLE I
CFD MODEL PARAMETERS AND INITIAL SETUP CONDITIONS

Parameter	Value
CFD Solver	Star-CCM+
Turbulence Model	$k-\omega$ SST
ΔT	0.001 s
$y+$	Blades: $1 < y+ < 100$ Nacelle: $y+ < 5$
Inlet Velocity	2 m/s
TSR	7
Ambient TI	0.05

TABLE II
DESCRIPTION AND NOTATION FOR THE 3 MODELLING CASES

Case Name	Description
ST	Single Turbine (ST) in the free stream
TT	Twin Turbines (TT) counter-rotating
TT+SS	Twin Turbines + Support Structure (TT+SS)

2) Case Setup: The turbines and the structure are modelled in 3D flow using the Computational Fluid Dynamics (CFD) software Star-CCM+. All model results reported are transient and feature a sliding mesh, and the domain is initialised using results from a converged steady-state Moving Reference Frame (MRF) model on the same mesh. The RANS $k-\omega$ SST turbulence model is used at a Δt =0.001 s timestep. This 0.001 s timestep is the equivalent of 2,212 timesteps per revolution, or 0.162° rotation per timestep. The structure is fully resolved with $y+ < 5$ and the sliding mesh turbine blades use adaptive y+ wall functions with $1 < y+ < 100$. The CFL number is kept below 1 for the stationary foundation and nacelle, as well as the blades surface, and is around 100 at the leading and trailing edge tips of the blades. An ambient TI of 0.05 was applied to the domain and kept constant across each simulation. A TI value of 0.05 would be lower than expected at a typical tidal site as seen in Ref. [15], however a low ambient TI% is adequate for this study and a full TI sensitivity study will be undertaken using collected ADCP data in future work. For all simulations, 10 full revolutions are simulated and the final 5 steady revolutions are used to take an average for readings. To reduce computational cost, all simulations are initialised with a converged steady-state RANS MRF model.

Three simulation cases are run and compared, detailed in Table II-B2. The Single Turbine (ST) model is used as a setup for model validation and is also used as a benchmark case to enable comparison for future models. Then, the Twin Turbines (TT) case uses a symmetry plane to simulate proximity to a neighbouring turbine, in counter-rotating formation with both turbines in the same phase. Finally, in the Twin Turbine + Support Structure (TT+SS) case, the wing section and vertical beams are added to the model to simulate two turbines operating in the wake of a multi-rotor foundation.

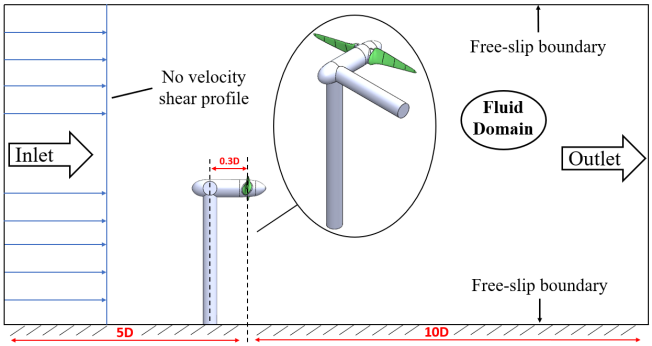

Fig. 2. Single wing domain with symmetry plane.

TABLE III
MODEL BOUNDARY CONDITIONS

Parameter	Distance	Definition
Inlet	5D	Velocity Inlet
Outlet	10D	Pressure Outlet
Bottom face	1.2D	Slip wall
Outer side face	7.5D	Slip wall
Top face	7.5D	Slip wall
Inner side face	7.5D*/0.65D^{+}	Slip wall/Symmetry Plane

*ST case, $^{+}$TT and TT+SS cases.

3) Domain Boundary Conditions: A simple schematic of the modelling domain for the TT and TT+SS cases can be seen in Fig. 2. The side boundary walls and top surface are located 7.5D away from the turbine to reduce boundary interference. The velocity inlet boundary is located 5D upstream, and the pressure outlet 10D downstream. The turbine is set at a hub height of 1.2D, and the symmetry plane face is set at 0.65D, to simulate a 0.3D tip clearance between rotors.

Model boundary conditions are summarised in Table II-B3. The ST model operates in the free stream and has no symmetry plane. This is introduced for the TT model and the TT+SS model, but all other aspects are kept consistent across the 3 models.

4) Mesh: Meshing was conducted through the Star-CCM+ internal parts-based meshing tool and model mesh independence was assessed using the Grid Convergence Index (GCI) method outlined in Ref. [16]. Table II-B4 displays each models final cell count. The turbine meshes within the rotational domain are identical across all 3 models for consistency. The difference in final cell count arises from the different boundary sizes between models, and in the case of the TT+SS model, accounts for the additional cells required to mesh the support structure. The final mesh is seen in Fig. 3.

Two structured inflation layers are used at each side of the rotating boundary interface to obtain a conformal interface between the rotating and stationary subdomains. Each blade's surface is also split into 5 sections to enable varying cell size across the length of the blade, with a larger density of cells towards the blade tip. The leading and trailing edges of the blades have are refined to accurately capture the curvature of the blade, and to preserve continuous inflation layering, especially around the sharp trailing edge. Fig. 3

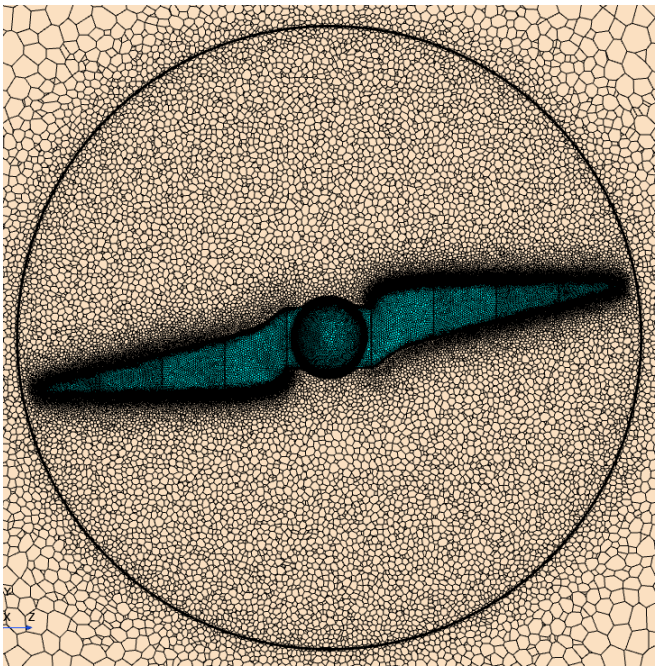

(a)

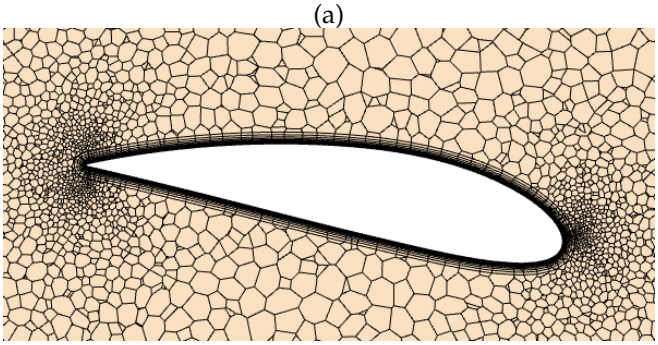

(b)

Fig. 3. Cross-sectional mesh images. (a) Turbine blades and rotational domain interface mesh. (b) Blade aerofoil cross-section with inflation layering and leading/trailing edge refinement.

TABLE IV
MESH CELL COUNTS FOR EACH MODELLING CASE

Model	Rotating cell #	Domain cell #	Total cell #
ST	6,413,579	934,459	7,348,038
TT	6,413,579	1,068,354	7,481,933
TT+SS	6,413,579	2,905,566	9,319,145

displays a cross-section mesh of a blade section at $0.6R$. The refinement at the leading and trailing edges of the blade can be clearly observed. The inflation layers extend for 14 layers, and the first layer thickness is sufficient to maintain $1 < y+ < 100$ across the blades. Inflation layers are structured cells with varying cell height used to capture boundary layer development near walls. Equivalent inflation layering is applied across the nacelle and is sufficiently small to produce a $y+ < 5$ for stationary parts. Additional mesh refinement extends $1D$ upstream of and $5D$ downstream of the turbine respectively.

Finally, mesh quality was assessed using internal Star-CCM+ tools to check cell quality and face validity, and to ensure that there were no chevroned cells present anywhere across the domain.

TABLE V
COMPUTATIONAL RESOURCE REQUIRED FOR THE ST MODEL SIMULATION

Parameter	Value
HPC	Archie-WeST
Nodes	1
Cores	40 per node
RAM	192 GB per node
Core-hours	≈14,400

C. Computational Resource

Simulations were run on the Archie-WEST HPC on a single 40-core node and the ST model case used approximately 14,400 core-hours per simulation. Simulating a single revolution took around 1,440 core-hours, equating to approximately 36 hours real time with a full simulation taking 15 days. The more intensive TT+SS case used approximately 18,400 core-hours and took around 19 days for a full simulation. The current fidelity of the simulations in terms of mesh $y+$ size and ΔT is governed by these computational limitations.

The computational resources used for the ST model simulation are detailed in Table II-C.

III. RESULTS

A. Validation

The data used for model C_P validation is a set of direct measured samples from a full scale Tocardo T2 turbine test conducted by Tocardo at the European Marine Energy Centre (EMEC) in 2017. The data measurements are also accompanied by an in-house BEMT model developed by Tocardo of their T2 turbine. The floating device was equipped with ADCP's for measuring flow velocity, and the C_P data set values were back calculated from turbine torque and flow velocity readings. The normalised values can be seen in Fig. 4. The data is scattered and noisy but this is expected from measured data in real life conditions. There are many differences between the measured data and what is actually modelled, mainly due to turbulence intensity and potential flow misalignment. Nevertheless, this dataset provides a foundation for validation of the model C_P vs TSR curve which shows good agreement on both the peak TSR of 7 and the overspeed TSR range.

B. Turbine power performance

Fig. 5 (b) shows the turbine blades in the shadow of the support structure wing section, causing the drop in generated torque.

The C_P for the TT case and the TT+SS case over a single revolution are seen in Fig. 6. These values are normalised against the ST case used as a benchmark value.

The C_P for the ST case is a constant value as expected for a model without any velocity gradient or boundary interference. All C_P values are normalised against the mean value for the ST model. Slight instability in this value can be attributed to the ambient turbulence present in the domain.

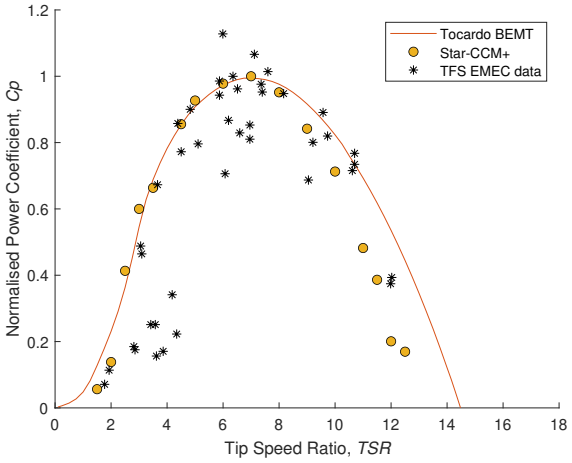

Fig. 4. MRF CFD validation against TFS EMEC measured data and Tocardo BEMT.

For the TT model, the C_P signal oscillates sinusoidally throughout the revolution. The TT case fluctuations can be attributed to interference with the adjacent turbine as the blades approach each other at 0° and 180° in the revolution. C_P fluctuates by 0.9% which is 0.45% above and below the mean value for C_P, with the C_P increasing to its max value when the blades from the adjacent turbines are closest together.

For the TT+SS case, the influence of the structure shadowing on power performance is clear. As the blades pass the structure, the C_P is reduced by $\approx 30\%$ before returning to its mean value. The largest drop in C_P occurs as the blades pass the structure beams, with some slight variation of a few % in magnitude. As the blades pass through the structure wake, the generated torque temporarily decreases which induces this drop in C_P. Across a revolution, this equates to an effective drop in mean C_P of $\approx 8\%$ when compared to the benchmark value set from the ST model case used for comparison.

C. Turbine blade loading

The blade load polar plots display the azimuthal variation in thrust load for the TT case and the TT+SS case through a single revolution. Fig. 7 shows the normalised thrust and power loading for the TT case.

The impact and interference effects due to turbine proximity are visible in the TT polar plot. Here, the turbine blades are horizontal at 0° and 180°, and are vertical at 90° and 270°. As the inner blades from adjacent turbines approach each other, a slight blade thrust load increase is observed due to the additional interference, increasing the torque. The increases in thrust are seem at around 15° and 195°. As the blades move outward again the thrust returns to its mean value. Interestingly, it is observed that the turbine power generated seems to lag the peak thrust point by approximately 30°. During a revolution, the thrust peaks first, and then the power follows.

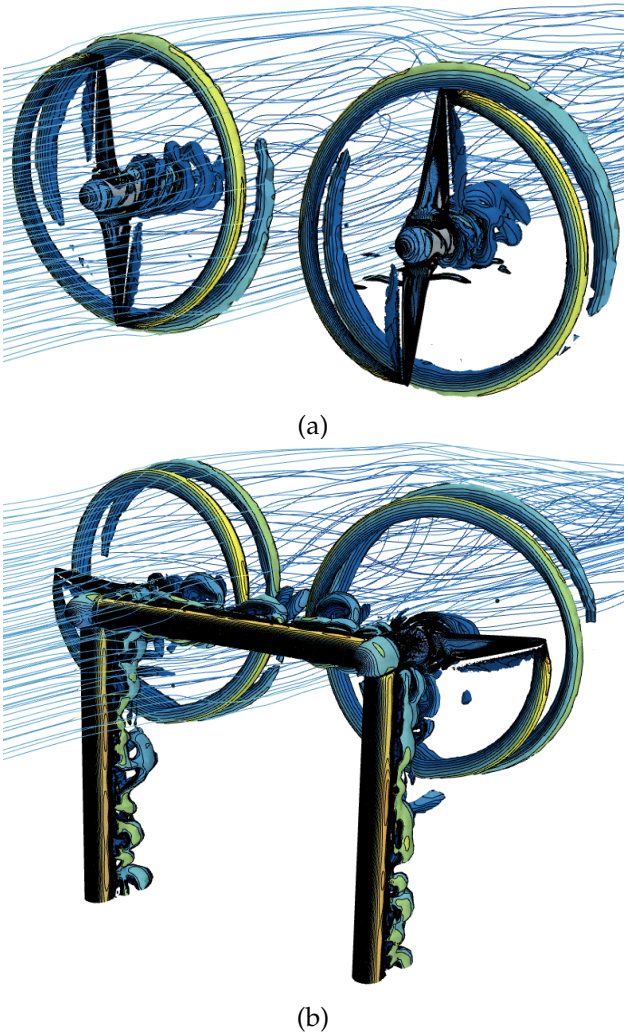

Fig. 5. Isosurface vorticies and streamlines. (a) The TT model case with blades in the vertical position. (b) TT+SS model case with the blades in the horizontal position, in the shadow of the wing section.

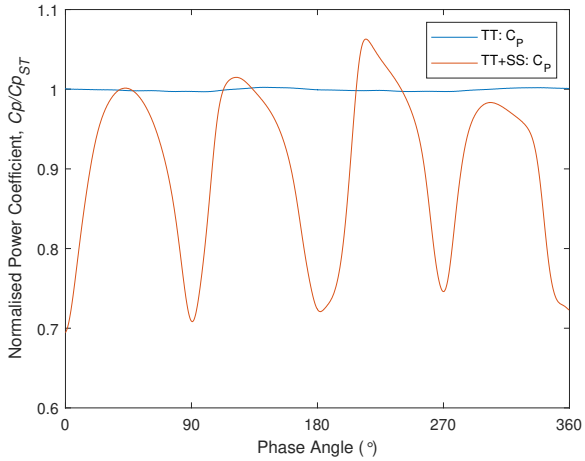

Fig. 6. Power coefficient for the TT and the TT+SS models normalised against the ST model over a single revolution.

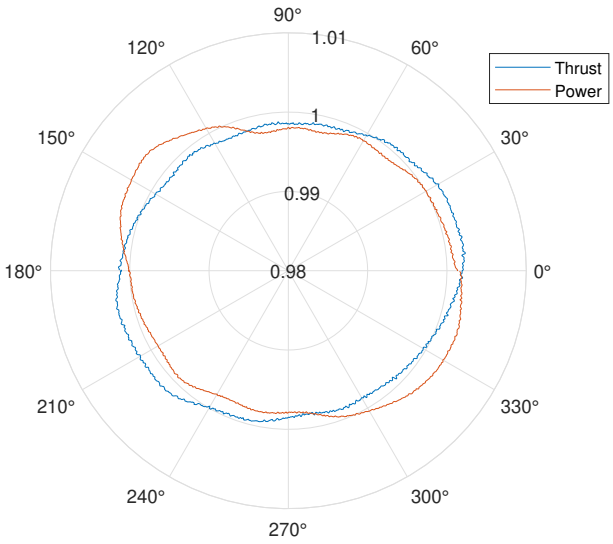

Fig. 7. Thrust and power values for the TT case normalised against the ST model.

The thrust load on the inner most blades is higher than the outer blades due to the increased blockage between the turbines causing a disparity in blade loading. When considering a single turbine, the load on the inner most blade is $\approx 1.4\%$ higher than the outer blade when the turbine is at 0° or 180° phase angle, which is when both turbines blades are closest together.

Other studies have designed for constructive interference, and optimised turbine spacing to achieve additional power output in channelled flows with high local blockage ratios. Here, the turbines are operating in an open flow condition, with low blockage ratios, but the impact due to local interference from adjacent turbine proximity can still be seen.

Fig. 8 then displays the same plot for the TT+SS case. The same plot for the TT case from Fig. 7 is included again for reference and comparison between the two cases.

The impact of the multi-rotor foundation on blade loading through a single revolution is clearly visible in this plot. At this scale, the oscillations due to adjacent turbine interference, seen in the TT model, are overshadowed by the impact of the foundation shadow effect that is present in the TT+SS case. The largest fluctuations in thrust occur as the turbine blades pass through the structure shadow where there is a velocity deficit and the loading on the blades temporarily subsides. This can be seen at 0°, 270°, 180°, and 90°, and is responsible for $\approx 20\%$ fluctuation in normalised C_T loading.

D. Turbine loading frequencies

Fig. 9 displays the FFT plot for Torque and Thrust for both the TT and the TT+SS models.

The 1st peak occurs at 0.45 Hz and is the $1p$ frequency occurring once per revolution and due to the turbines angular velocity, this peak is seen in both models. The 2nd peak is then the 0.91 Hz peak which is the $2p$, occurring twice per revolution. This frequency corresponds to the thrust and torque peaks discussed in Section III-C, and some contribution from the tower shadow effect in the TT+SS model. This is the most significant frequency for the TT model when we are considering two turbines in isolation. The largest peak is seen at 1.82 Hz for the TT+SS model, which corresponds to a quarter of the rotational speed.

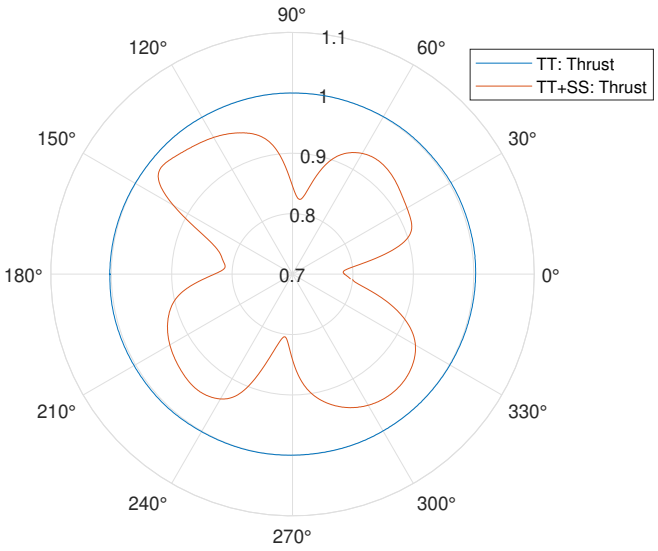

Fig. 8. Thrust for the TT+SS case with the previous TT case included for reference, normalised against the ST model.

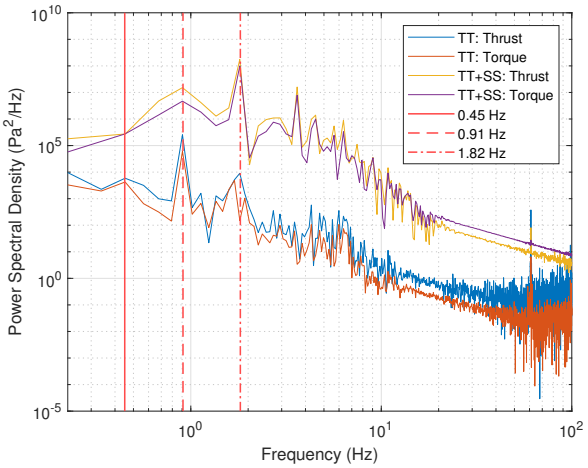

Fig. 9. Thrust and Torque loading frequencies for both the TT and TT+SS models.

This will be the sum of the shadow effect from both the vertical beam and the wing beam as there are 2 main foundation members and 2 turbine blades. This is the largest magnitude peak caused by the multi-rotor foundation shadowing effect which will only be present in every other tidal cycle when the turbines are downstream of this foundation. Additional peaks are harmonics of this main peak, most significantly the peak at 1.82 Hz.

Noise at the higher frequency range can partially be attributed to the ambient turbulence intensity throughout the domain and model unsteadiness.

IV. Discussion

Results presented in this paper give an insight into the approximate scale of the loading that could be expected when operating turbines in the wake of a multi-rotor foundation, and highlight that turbine operating conditions should be an important consideration for developers.

Three distinct operating scenarios were considered to investigate turbine power performance and loading implications when a multi-rotor foundation is used to house two counter-rotating, 2-bladed tidal turbines. It was found that the addition of the multi-rotor structure induced a $\approx 20\%$ fluctuation in blade thrust loading and turbine power generation at a 1.82 Hz frequency during operation when the turbines are downstream of the support structure. This drop in thrust and torque occurs each time the blades pass through the structure wake, resulting in an effective $\approx 8\%$ drop in mean C_P when comparing with the ST benchmark case.

It was additionally observed that when operating two adjacent turbines in isolation, in the TT case, that a $\approx$ 1.4% fluctuation in blade thrust loading would occur at a 0.91 Hz frequency due to adjacent turbine interference as blades from opposing turbines approached each other. The mean C_P for the TT case would oscillate about the mean value set in the ST benchmark model.

The spectral density magnitude of the peaks for the TT+SS model are significantly greater than for the TT model, as can be seen comparing models in Fig. 9. The difference in peak magnitude is most significant for the 1.82 Hz frequency peak, which has the greatest magnitude for the TT+SS model due to the tower shadowing effect but is mostly just a harmonic of the 0.91 Hz peak in the TT model. It is this difference which will contribute the most to fatiguing on the blades and is an area that requires more investigation to increase understanding of the relationship between turbines and multi-rotor foundation.

To enable the initial stage of this study so far, many assumptions and simplifications have been made. As reported in previous studies and literature comparisons between CFD RANS and LES turbulence models, RANS is able to model blade forces and coefficients accurately, but is insufficient for capturing detailed vortex shedding frequency. Therefore, the contribution of vortex shedding must be considered in future work as part of this project in the continued development of the model to increase the fidelity and include the LES turbulence model so that the desired responses can be resolved.

The simplifications in the modelling physics setup must be addressed to increase confidence in the modelling process, which would require reducing the model $y+$ and CFL number. The initial results presented here indicate that the foundation induced shadowing effect may have a significant impact on turbine cyclic loading and fatigue life, and justify further work modelling work on the topic at a higher fidelity scale and computational cost. Additionally, the model results so far are known to vary with TI%, therefore various turbulence intensities will be considered, and velocity gradients modelled using collected site specific ADCP data for realistic TI% values and gradients. Further modelling work should also consider the foundation members separately to better understand the contribution that each one contributes.

V. Conclusion

Three modelling cases were set up and simulated to assess the impact that a the shadow from a multi-

rotor support structure has on turbine performance and loading. These ST case modelled a single turbine operating in the free stream, the TT case modelled two adjacent, counter-rotating turbines, and the TT+SS case considered the same two turbines downstream of the multi-rotor support structure. It was found that operating turbines downstream from the support structure could lead to an $\approx 30\%$ fluctuation in C_P and an $\approx 20\%$ fluctuation in C_T loading on the blade, occurring at a 1.82 Hz frequency. These fluctuations would result in an $\approx 8\%$ drop in mean C_P during device operation and additional sources of cyclic blade loading, contributing to fatigue. This demonstrates a substantial, non-negligible contribution of the support structure, which must be accounted for, particularly on multi-rotor devices that include multiple members of support that could interfere with the flow upstream of the rotor.

Steady-state MRF models were validated against measured data and used to initialise the transient solutions. The CFD software Star-CCM+ was used with the RANS $k-\omega$ SST turbulence model at a $\Delta t = 0.001$ s timestep for the transient models, simulating 10 full revolutions for each case. The work presented here provides evidence for key turbine and support structure interactions. Future work should build on this foundation by further quantifying the impact that these fluctuating loads could have on the fatigue life of turbine blades, as well as implications on annual energy production and LCOE. Mitigation techniques to reduce support structure impact on turbine performance should be considered and explored. Higher fidelity simulation models which could capture structure vortex shedding could be used to investigate Vortex Induced Vibrations (VIV) through the support structure and turbines. Tank testing would enable further investigation into the dynamic of flow past a support structure and may be required for future model validation.

ACKNOWLEDGEMENT

B. Townley thanks HydroWing for project data and technical support; the EPSRC and NERC for project funding through the IDCORE programme; Rachael Smith and Allan Mason-Jones for technical support with the MRF model development. Results were obtained using ARCHIE-WeSt High Performance Computer (www.archie-west.ac.uk).

REFERENCES

[1] J. McNaughton, B. Cao, C. R. Vogel, and R. H. J. Willden, "Model scale testing of multi-rotor arrays designed to exploit constructive interference effects," *Proceedings of the 13th European Wave and Tidal Energy Conference*, 2019.

[2] J. McNaughton, S. Ettema, F. Zilic de Arcos, C. Vogel, and R. Willden, "An experimental investigation of the influence of inter-turbine spacing on the loads and performance of a co-planar tidal turbine fence," *Journal of Fluids and Structures*, vol. 118, p. 103844, 2023. [Online]. Available: https://doi.org/10.1016/j.jfluidstructs.2023.103844

[3] D. R. Noble, S. Draycott, A. Nambiar, B. G. Sellar, J. Steynor, and A. Kiprakis, "Experimental assessment of flow, performance, and loads for tidal turbines in a closely-spaced array," *Energies*, vol. 13, no. 8, 2020.

[4] C. E. Badoe, M. Edmunds, A. J. Williams, A. Nambiar, B. Sellar, A. Kiprakis, and I. Masters, "Robust validation of a generalised actuator disk CFD model for tidal turbine analysis using the FloWave ocean energy research facility," *Renewable Energy*, vol. 190, pp. 232–250, 2022. [Online]. Available: https://doi.org/10.1016/j.renene.2022.03.109

[5] I. Afgan, J. McNaughton, S. Rolfo, D. D. Apsley, T. Stallard, and P. Stansby, "Turbulent flow and loading on a tidal stream turbine by LES and RANS," *International Journal of Heat and Fluid Flow*, vol. 43, pp. 96–108, 2013. [Online]. Available: http://dx.doi.org/10.1016/j.ijheatfluidflow.2013.03.010

[6] C. Frost, C. E. Morris, A. Mason-Jones, D. M. O'Doherty, and T. O'Doherty, "The effect of tidal flow directionality on tidal turbine performance characteristics," *Renewable Energy*, vol. 78, pp. 609–620, 6 2015.

[7] G. E. Suhri, A. Rahman, L. Dass, and K. Rajendran, "The influence of tidal turbine arrangement on the wake interaction in shallow water," *Journal of Physics: Conference Series*, vol. 2051, no. 1, 2021.

[8] D. Coles, A. Angeloudis, D. Greaves, G. Hastie, M. Lewis, L. MacKie, J. McNaughton, J. Miles, S. Neill, M. Piggott, D. Risch, B. Scott, C. Sparling, T. Stallard, P. Thies, S. Walker, D. White, R. Willden, and B. Williamson, "A review of the UK and British Channel Islands practical tidal stream energy resource," 2021.

[9] B. Sanderse, S. P. Van Der Pijl, and B. Koren, "Review of CFD for wind-turbine wake aerodynamics," Tech. Rep.

[10] L. Mackie, P. S. Evans, M. J. Harrold, T. O'Doherty, M. D. Piggott, and A. Angeloudis, "Modelling an energetic tidal strait: investigating implications of common numerical configuration choices," *Applied Ocean Research*, vol. 108, 3 2021.

[11] F. Zahle, N. N. Sørensen, and J. Johansen, "Wind turbine rotor-tower interaction using an incompressible overset grid method," *Wind Energy*, vol. 12, no. 6, pp. 594–619, 2009.

[12] Z. U. Rehman, S. Badshah, A. F. Rafique, M. Badshah, S. Jan, and M. Amjad, "Effect of a support tower on the performance and wake of a tidal current turbine," *Energies*, vol. 14, no. 4, 2 2021.

[13] B. Guo, D. Wang, X. Zhou, W. Shi, and F. Jing, "Performance evaluation of a tidal current turbine with bidirectional symmetrical foils," *Water (Switzerland)*, vol. 12, no. 1, 2020.

[14] M. Reiso, T. R. Hagen, and M. Muskulus, "A calibration method for downwind wake models accounting for the unsteady behaviour of the wind turbine tower shadow behind monopile and truss towers," *Journal of Wind Engineering and Industrial Aerodynamics*, vol. 121, pp. 29–38, 2013. [Online]. Available: http://dx.doi.org/10.1016/j.jweia.2013.07.016

[15] I. A. Milne, R. N. Sharma, R. G. Flay, and S. Bickerton, "Characteristics of the turbulence in the flow at a tidal stream power site," *Philosophical Transactions of the Royal Society A: Mathematical, Physical and Engineering Sciences*, vol. 371, no. 1985, 2013.

[16] I. B. Celik, U. Ghia, P. J. Roache, C. J. Freitas, H. Coleman, and P. E. Raad, "Procedure for estimation and reporting of uncertainty due to discretization in CFD applications," *Journal of Fluids Engineering, Transactions of the ASME*, vol. 130, no. 7, pp. 0 780 011–0 780 014, 2008.